Segmentation of urban built up area using Fisher discriminant analysis, intensity and vegetation strength of Landsat images

JORGE LIRA and LOURDES HIDALGO
Instituto de Geofísica
Universidad Nacional Autónoma de México
Cd. Universitaria
04510 México DF, México

Abstract: - A series of studies in urban growth involve the segmentation of urban built up area. This segmentation may used as input to geospatial models to quantify and map urban growth. The segmentation may be used as well to study the dynamics of urban growth on a certain time span. We present in this work a method to segment urban built up area from Landsat multi-spectral images. Our method uses the expansion of the image in terms of three variables: intensity, vegetation strength and fisher discriminant analysis. These variables are input into a c-means fuzzy classier. From this classifier, a binary image, named the bitmap, is derived. The bitmap is a logic state image where the state ON is related to city pixels, and the state OFF to non-city pixels. A case of study is presented that comprised one of the largest cities of the world with a high dynamic growth and high urban built up density: México City. A set of images that cover a time span of eleven years is considered. The field data consist of a detailed map and field work.

Key-Words: - Segmentation, urban built-up, urban morphology

1 Introduction

A number of applications of urban studies require the segmentation of the urban built up area; the scientific literature shows a variety of methods of urban segmentation since more than twenty years. In one of the earliest works on urban segmentation, a set of texture operators were applied to a high resolution urban scene [1]. Several urban features were classified on the grounds of a supervised texture classifier based on a co-occurrence matrix and six texture measures. With the use of map information as a training field, an iterative feedback algorithm based on Markov potential was developed to segment the urban area of the city of Calais, France [2]. A classification of the urban built up area according to its density was achieved using a co-occurrence matrix [3]. This co-occurrence matrix is applied to a binarized image of the urban built up area, and a classification map of three densities is obtained by means of a supervised classification. A classification of urban area using support vector machine (SVM) was obtained on an ASTER multi-spectral image of the area of Beer Sheva, Israel [4]. In this classification, several city features were differentiated. Morphological information about the various elements that compose an urban area may be derived on the grounds of morphological transformations [5]. These transformations are used to generate a differential morphological profile of the urban built up area. Spectral classification may be used as well to determine urban land cover [6], [7]. However, significant limitations are found for available multi-spectral sensors, hence, resulting in low accuracy classification of the urban environment. When additional information and fuzzy classification models are included, the classification accuracy may significantly increase. Visual classification of air photos and IKONOS images is used to segment urban built up areas [8]. With this segmentation, the spatial-temporal form of urban growth is studied and analyzed. In a different approach, both spectral and spatial heterogeneity are used to segment the image in a classification process [9], [10]. With this method, to improve urban characterization, multi-temporal and multi-angle images may used as well. Synthetic aperture radar (SAR) images may be used in the task that leads to an improvement of classification accuracy of land cover class in an urban area [11]. The segmentation of urban area is required to establish models of urban growth. The evolution trends of the Tunis Metropolitan Area has been done using SPOT XS images by extracting land cover by identification of major urbanization process [12].

In this research we propose an expansion of a multi-spectral Landsat TM image in terms of three variables resulting from, intensity, vegetation strength and fisher discriminant analysis of urban built up. These three variables are sufficient to characterize the complex spatial extension of the urban built up of Mexico City. The objectives of this work are three fold: (a) to model urban built up spatial extension, (b) to produce a segmentation of a major urban area and, (c) to evaluate basic morphological parameters of the segmented urban area.

2 Materials and Methods

In this section we describe the multi-spectral satellite images used to segment a major urban area, and we provide details on the methodology employed for this task. We give details as well about the field data used to validate our results.

2.1 Satellite images

A set Landsat TM multi-spectral images covering the urban area of Mexico City was selected to test the model proposed in this work. The path/row of these images is 26/47; the acquisition dates are: March 7, 1989, May 24, 1991, November 21, 1993, February 20, 1998, February 23, 1999, and March 21, 2000. From each image, a sub-set of 2883 × 2964 pixels was extracted and geocoded to UTM projection and resampled to a pixel size of 28.5 × 28.5 m^2. From now on, this sub-set will be referred as the image. Band 5 of the image of year 1998 shows the study area in Fig. 1.

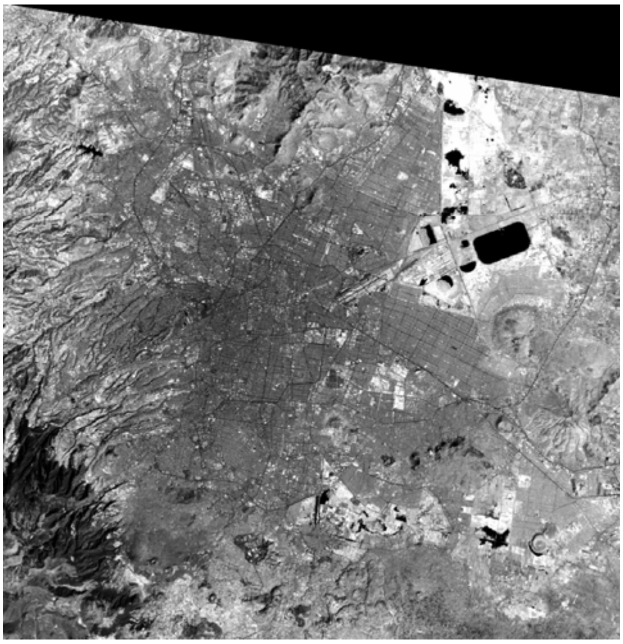

Figure 1.- Band 5 of image of February 20, 1998.

A description of the study area is as follows. The image, named Mexico City, shows most of the metropolitan area of the third largest city in the world. This scene includes the following features: (i) a forest zone to the southwest of the city where patches of pine trees are appreciated; the patches are intermingled with deforested areas (ii) numerous agriculture fields to the south and to the west, and, (iii) a group of small satellite towns to the south. The vegetation cover types are very much altered by the pressure of the urban growth and anthropogenic activities. Vegetation types include pines, oaks, shrubs, grass and various agriculture cover types. Several water bodies are visible to the northeast of the metropolitan area. Mexico City has experienced a rapid expansion growth in the last twenty years. A segmentation method is required to examine the morphology of such growth.

2.2 Map of the city

Six maps that cover the urban area of Mexico City were acquired. A mosaic from such maps was prepared that cover most of the metropolitan area of Mexico City. These maps were elaborated in the year 1997 from aerial photographs by using photointerpretation methods. These maps are produced and commercialized by the National Institute of Geography, Statistics and Informatics (INEGI) of Mexico. In addition to these maps, field work upon selected places of the city was undertaken. This mosaic was used to asses the goodness of the segmentation of the image of February 20, 1998. Less than one year difference span between the acquisition of this image and the production of the maps. The field work corroborated that changes in the city in this time span are insignificant for the scale and detail discerned by the Landsat image. This mosaic is the only one available for the acquisition dates of the images used in this research.

2.2 Segmentation model

An expansion of the multi-spectral image set is proposed in terms of the variables mentioned in the introduction; details of the usefulness of these variables in the segmentation procedure are provided below.

2.3.1 Fisher discriminant analysis

The complex spatial extent of a city contains many spectral elements that may confuse with non-city elements surrounding the urban built up area [6]. The highest confusion comes from the high spectral reflectivity of the buildings and exposed bare soil; a spectral classification study conducted in this research confirms this confusion. To lessen the confusion of the city elements with urban surroundings a Fisher discriminant analysis was carried out. Fisher analysis, known as well as canonical analysis [13], is expressed in the following way. Let f(**r**) be a multi-spectral image formed by η - bands. Let $\xi = \{a, b, \ldots k\}$ be a set of k spectral classes determined by means of training fields. Let $\mathbf{K}_j^f$ be the covariance matrix of the j^{th} - class of such set. We form the average covariance matrix of such classes as

$$\mathbf{K}_{av}^{f} = \frac{1}{N_k} \sum_{j=1}^{N_k} \mathbf{K}_j^f \qquad (1)$$

Where N_k is the number of classes in the set. In addition to this, let us define $\mathbf{K}_{am}^{f}$ as the covariance matrix among classes

$$\mathbf{K}_{am}^{f} = \frac{1}{N_k - 1} \sum_{j=1}^{N_k} (\boldsymbol{\mu}_j - \boldsymbol{\mu}_0)(\boldsymbol{\mu}_j - \boldsymbol{\mu}_0)^t \qquad (2)$$

Where the centroid $\boldsymbol{\mu}_0$ is calculated with the following formula

$$\boldsymbol{\mu}_0 = \frac{1}{S_n} \sum_{j=1}^{N_k} N_j \boldsymbol{\mu}_j \qquad (3)$$

The vector $\boldsymbol{\mu}_i$ is the mean of the i^{th} - class and N_i its population. The total population of the set ξ is S_n. To achieve maximum spectral separability among the classes defined in the set ξ we use the generalized eigenvalue equation

$$[\mathbf{K}_{am}^{f} - \Lambda \mathbf{K}_{av}^{f}]\mathbf{D} = 0$$

Since the matrices $\mathbf{K}_{am}^{f}$, $\mathbf{K}_{av}^{f}$ and Λ are symmetric, this equation may be rewritten as

$$[(\mathbf{K}_{av}^{f})^{-1}\mathbf{K}_{am}^{f} - \Lambda \mathbf{I}]\mathbf{D} = 0 \qquad (4)$$

Therefore, the matrix **D** is a matrix formed by the eigenvectors of $(\mathbf{K}_{av}^{f})^{-1}\mathbf{K}_{am}^{f}$, and Λ is the matrix of eigenvalues. Such eigenvectors span an orthonormal coordinate system in terms of which an image can be expanded. The number of bands of the image that results from the application of equation (4) is $N_b = \min[\eta, N_k - 1]$ [13].

The Fisher discriminant analysis was applied to two classes: city and bare soil. The pixels related to these classes were obtained using an interactive polygon extraction process, which is acted upon a false color composite image displayed on a high resolution computer monitor. With such pixels, equation (4) was applied; since $N_k = 2$, the resulting image contains only one band. This is the first variable of our model: X_1.

2.3.2 Spectral intensity

The spectral intensity of urban elements (buildings, streets) is in general higher than the intensity in rural areas. The spectral intensity is therefore an element to discriminate the city from the rest of the image [14]. It is well understood that the first principal component is proportional to the spectral intensity of a scene [13]. The spectral intensity of the city is calculated according to the following rationale. A high density built up area of the city is determined; this is done with the help of field work and a city map. A set of pixels comprised in this area is extracted from the bands of the multi-spectral image. The principal component analysis is applied to such set of pixels and a kernel is obtained. This kernel is in turn applied to the whole image; the first component of this application is the spectral intensity of the city. This is the second variable of our model: X_2.

2.3.2 Vegetation strength

The area occupied by the urban built up is mostly deprived of vegetation. In this work we do not consider parks and green areas within the city as part of the urban built up. To measure the vegetation strength of the urban built up area and surroundings we use the band greenness of the Kauth - Thomas transformation (KT) [13]. This transformation may be written in vector form as

$$g(\mathbf{r}) = \mathcal{R} f(\mathbf{r}) \qquad (5)$$

For Landsat TM, the matrix $\mathcal{R}$ is formed by the vectors: a) that point along the principal diagonal which soils distributes, b) that point along the development of green biomass, and c) that point along the direction of vegetation maturity. There are three vectors more to complete a matrix $\mathcal{R}$ of 6×6 dimension; the infrared band of the image is not taken into account. In this sense, the KT transformation generates a multi-spectral image with six bands. However, in similar form as the principal component decomposition, only the first three bands carry significant information, the last three bands of the KT are formed mostly by noise. The above mentioned directions are defined in the feature space formed by the bands of the multi-spectral image. Since a Landsat TM image carries an intrinsic dimensionality of three, the first three vectors are enough to account for the information content of the image. The greenness band is a vegetation index that reflects the fact that the urban built up is deprived of vegetation. This index is selected to cancel the effect of the background soil and city brightness from the output vegetation index image. The band greenness is the third variable of our model: X_3.

The above methodology leads to the derivation of the set of variables $\{X_1, X_2, X_3\}$. None of these variables can account by itself to produce a clear segmentation of the urban built up area. Some confusion may arise, i.e., some elements of the rural areas such as forest, agriculture, or bare soil may show similar values of spectral intensity, or vegetation strength as the elements of the city. Therefore, these three variables must be taken concurrently to avoid confusion on the segmentation of the city area. This leads to the expansion of the image in terms of three variables. To show that the set of variables $\{X_1, X_2, X_3\}$ generates an enhancement of the urban built up; we use multivalued probabilistic logic [15] which combines these variables according to the following formula

$$X = 1 - \prod_{i=1}^{3} (1 - X_i) \qquad (6)$$

Fig. 2, shows the image X; a clear enhancement of the city is observed in this figure with respect to band 5 of the image of February 20, 1998 (Fig. 1).

2.4 Generation of the bitmap

The variables $\{X_1, X_2, X_3\}$ are input into a fuzzy c-means algorithm from which a split-and-merge procedure is applied until a two class-image is obtained: city and non-city [16]. The fuzzy clustering procedure was initiated with 5 clusters and tested thereafter in increments of 5 clusters until a clear segmentation was obtained with minimum computing time; 30 clusters was the best number for this task. In a second step, the clusters related to the urban built up area were identified and merged together; the rest of the clusters were readily merged into one cluster. In a third step, a binary image was determined with, the logic state ON corresponding to the city, and the logic state OFF to the rest of the image; this image is named the bitmap of the city. Fig. 3 depicts the bitmap achieved with the clustering procedure applied to the image of February 20, 1998.

Figure 2.- Combination of variables X_1, X_2, X_3.

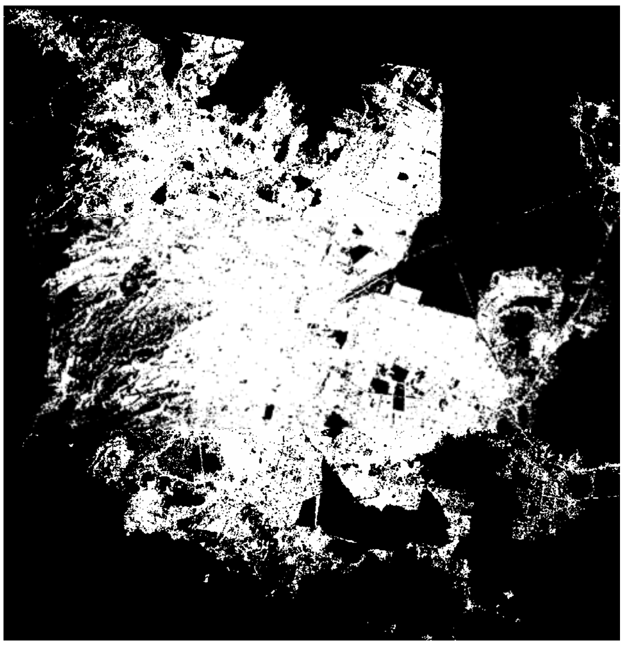

Figure 3.- Bitmp of image of February 20, 1998.

To eliminate isolated pixels from the segmentation, a hit or miss morphological operation was applied to the bitmap [17]. Once the bitmap is obtained, basic morphological parameters may be derived. With the use of the FragStat computer code, the area and the fractal dimension were calculated for the image set [18]. We run the FragStat software under conectivity – 8. The fractal dimension is related to the scale defined by the image pixel size. The area is the accumulated value of all the patches of the landscape covered by the bitmap. Fig. 4 shows the evolution of the area and Fig. 5 depicts the fractal dimension of 1,200 largest patches for each image of the set. A slight increase of the fractal dimension is observed for the largest patches.

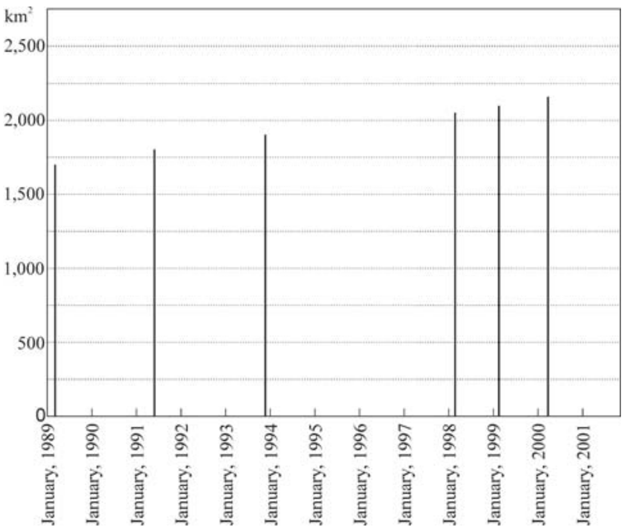

Figure 4.- Evolution of the area of Mexico City.

3 Results

A logic AND between figures 1 and 3 produces the segmentation of the urban built up area. To test the validity of this result, a detailed comparison with a map was undertaken; selected visits to a number of spots in the city were carried out as well. In order to provide an analysis of the results, an overlay of the map of the city with Fig. 3 was prepared (Fig. 6). The following aspects may be appreciated from Fig. 6: a) In general, the city limits defined by the map coincide with the segmentation, b) Parks, idle lots an open spaces with no buildings are not included in the segmentation as part of the urban built up area, c) Low density urban areas are detected by the segmentation as scattered points, d) Some confusion prevails in several parts of the study area were some spots (in white) detected by the segmentation do not actually belong to the city, and e) Some buildings not reported in the map are actually detected by the segmentation.

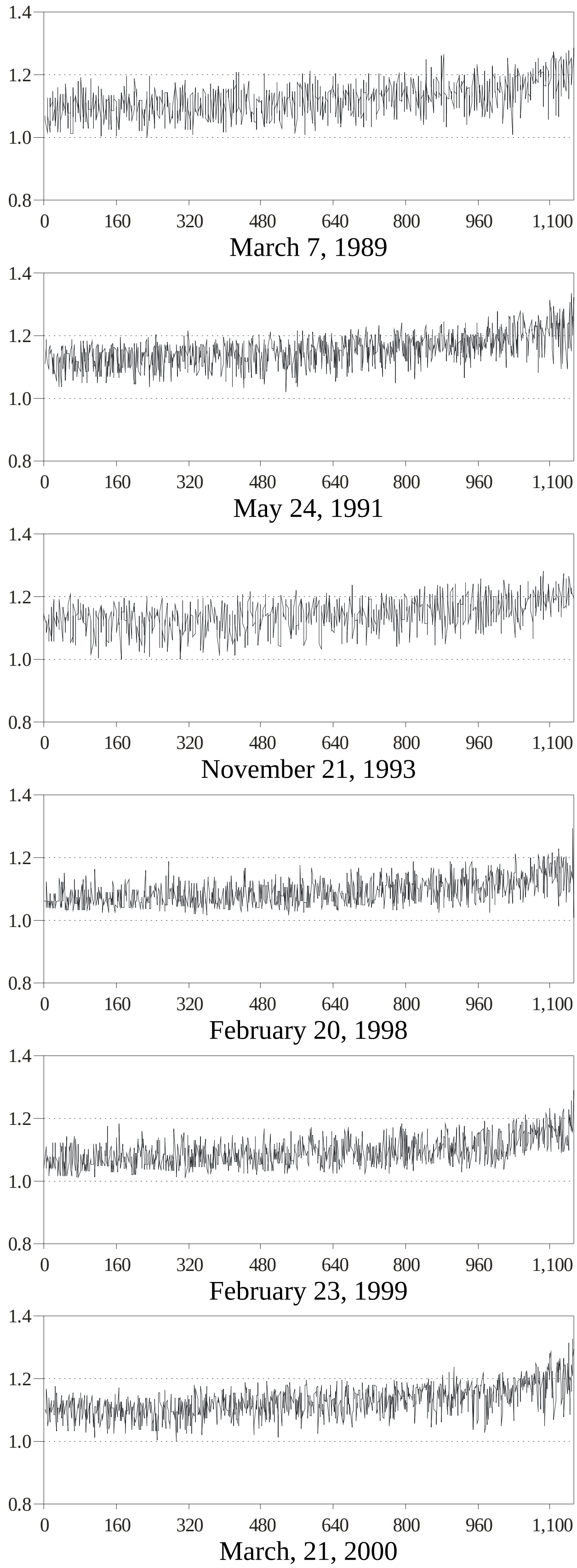

Figure 5.- Fractal dimension of the image set.

In order to develop a detailed discussion of our results, a number of amplifications of selected areas are shown in Fig. 6; in this figure, light gray indicates the segmentation achieved by our method, in dark gray the city limits determined by the map are identified.

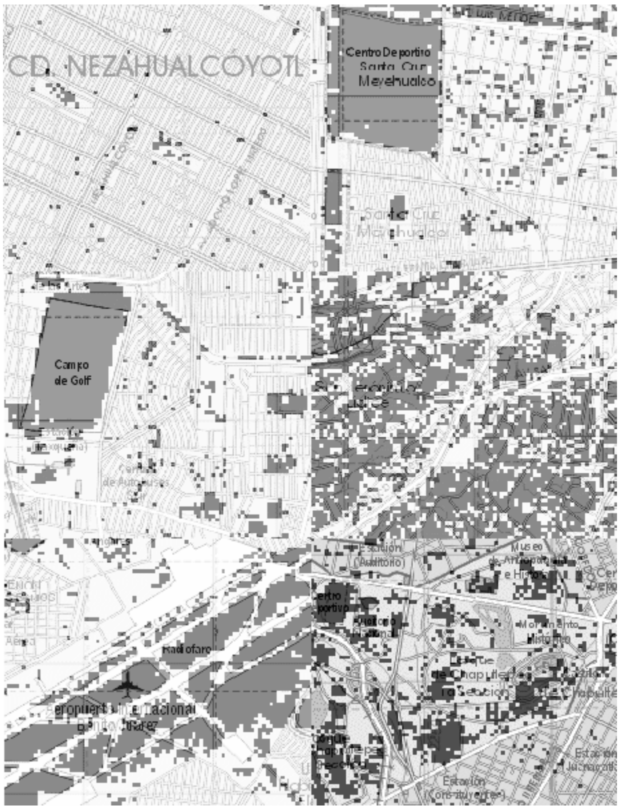

Figure 6.- Comparison of segmentation with city map.

(1) *High density urban area*
This amplification shows a portion of the city with high density constructions (upper-left); few parks and idle lots are appreciated. In these areas, the segmentation agrees well with the map; limits of the city are well defined. Small parks and idle lots are void, i.e., not included in the segmentation.

(2) *Medium density urban area and idle lot*
This portion of the image shows a medium density construction area with an idle lot in the center (upper-right). The frontiers of idle lots are well defined in the segmentation. In this area, the urban built up appears in the segmentation as high density scattered spots.

(3) *Medium density urban area and park*
This portion of the image shows a medium density construction area with a park on the left (middle-left). Parks are not considered as urban built up; therefore they are segmented and classified as non-city. The borders of parks are well defined. In this area, the urban built up appears in the segmentation as high density scattered spots; void spaces are associated with green areas.

(4) *Low density urban area*
This portion of the image shows a residential area with low density housing and ample spaces full of vegetation (middle-right). These areas appear in the segmentations as scattered points; void spaces are associated with parks and lawns.

(5) *Airport*
This portion of the image shows part of the airport of Mexico City (lower-left). The main building of the airport and the landing fields are detected as part of the urban built up area. The space between the landing fields is void meaning not belonging to the city.

(6) *Buildings not reported in the map*
A series of buildings not reported in the map are actually detected by the segmentation (lower-right). This is the case of a number of museums located in an amusement park; these buildings are clearly visible in this amplification as white spots; void spaces are associated to green areas.

4 Conclusion

One of the largest, high density and rapid expansion cities of the world has been segmented from a Landsat image. The built up area of this city is modeled in terms of three variables that describe its spectral behavior. These variables can be used as an expansion of the original image that depicts the area covered by the city. The expansion variables of the image are introduced into a c-means fuzzy clustering procedure by means of which a bitmap is prepared. To evaluate the quality of our segmentation, the bitmap was compared with a city map obtained from aerial photographs; field work was also done. This comparison agrees well with a map prepared within one year of the image acquisition date; this agreement is documented in relation to the detail and scale provided by the Landsat TM image employed in this research. The evolution of the area shows a steady increase and the distribution of fractal dimension indicates that the group of urban patches forms a set of fractal features. The fractal dimension of the largest city patches shows a similar distribution regardless of the area increase experimented by the urban built up.

Acknowledgment - This research was funded by project IN 113505 of DGAPA-UNAM.

References:

[1] Conners, R.W., Trivedi, M.M., and Harlow, Ch.A., Segmentation of a High-resolution Urban Scene Using Texture Operators, *Computer Vision, Graphics, and Image Processing*, Vol. 25, 1984, pp. 273 – 310.

[2] Yu, S., Berthod, M., and Giraudon, G., Toward Robust Analysis of Satellite Images Using Map Information – Application to Urban Area Detection, *IEEE Transactions on Geoscience and Remote Sensing*, Vol. 37 , 1999, pp. 1925 – 1939.

[3] Karathanassi, V., Iossifidis, Ch., and Rokos, D., 2000, A Texture-Based Classification Method for Classifying Built Areas According to Their Density, *International Journal of Remote Sensing*, Vol. 21, 2000, pp. 1807 – 1823.

[4] Zhu, G., and Blumberg, D.G., Classification Using ASTER Data and SVM Algorithms; The Case Study of Beer Sheva, Israel, *Remote Sensing of Environment*, Vol. 80, 2002, pp. 233 – 240.

[5] Benediktsson, J.A., Pesaresi, M., and Arnason, K., Classification and Feature Extraction for Remote Sensing Images From Urban Areas Based on Morphological Transformations, *IEEE Transactions on Geoscience and Remote Sensing*, Vol. 41, 2003, pp. 1940 – 1949.

[6] Herold, M., Gardner, M.E., and Roberts, D.A., Spectral Resolution Requirements for Mapping Urban Areas, *IEEE Transactions on Geoscience and Remote Sensing*, Vol. 41, 2003, pp. 1907 – 1919.

[7] Lu, D., and Weng, Q., Urban Classification Using Full Spectral Information of Landsat ETM+ Imagery in Marion County, Indiana, *Photogrammetric Engineering & Remote Sensing*, Vol. 71, 2005, pp. 1275 – 1284.

[8] Herold M., Goldstein, N.C., and Clarke, K.C., The Spatiotemporal Form of Urban Growth: Measurement, Analysis and Modeling, *Remote Sensing of Environment*, Vol. 86, 2003, pp. 286 – 302.

[9] Shackelford, A.K., and Davis, C.H., A Hierarchical Fuzzy Classification Approach for High-Resolution Multispectral Data Over Urban Areas, *IEEE Transactions on Geoscience and Remote Sensing*, Vol. 41 (9), 2003, pp. 1920 – 1932.

[10] Shackelford, A.K., and Davis, C.H., A Combined Fuzzy Pixel-Based and Object-Based Approach for Classification of High-Resolution Multispectral Data Over Urban Areas, *IEEE Transactions on Geoscience and Remote Sensing*, Vol. 41, 2003, pp. 2354 – 2363.

[11] Dell'Acqua, F., Gamba, P., and Lisini, G., Improvements to Urban Area Characterization Using Multitemporal and Multiangle SAR Images, *IEEE Transactions on Geoscience and Remote Sensing*, Vol. 41, 2003, pp. 1996 – 2004.

[12] Weber, C., and Puissant, A., Urbanization Pressure and Modeling of Urban Growth: Example of the Tunis Metropolitan Area, *Remote Sensing of Environment*, Vol. 86, 2003, pp. 341 – 352.

[13] Richards, J.A., and Jia, X., 1999, *Remote Sensing Digital Image Analysis, An Introduction*, Springer-Verlag, 1999.

[14] Hu, X, Tao, C.V., and Prenzel, B., Automatic Segmentation of High-Resolution Satellite Imagery by Integrating Texture, Intensity, and Color Features, *Photogrammetric Engineering & Remote Sensing*, Vol. 71, 2005, pp. 1399 – 1406.

[15] Nilsson, N., Probabilistic Logic, *Artifical Intelligence*, Vol. 28, 1986, pp. 71 – 87.

[16] Höppner, F., Klawonn, F., Kruse, R., and Runkler, T., *Fuzzy Cluster Analysis*, John Wiley & Sons Inc., 2000.

[17] Pratt, W.K., *Digital Image Processing*, John Wiley & Sons Inc., 2001.

[18] http://www.umass.edu/landeco/research/